Article:

Mazzini, I. orcid.org/0000-0003-2164-7826, Cronin, T.M., Gawthorpe, R.L. orcid.org/0000-0002-4352-6366 et al. (9 more authors) (Cover date: 1 August 2023) A new deglacial climate and sea-level record from 20 to 8 ka from IODP381 site M0080, Alkyonides Gulf, eastern Mediterranean. Quaternary Science Reviews, 313. 108192. ISSN 0277-3791

https://doi.org/10.1016/j.quascirev.2023.108192

A New Deglacial Climate and Sea-level Record from 20 to 8 ka from IODP381 Site M0080, Alkyonides Gulf, eastern Mediterranean

Ilaria Mazzini[1], Thomas M. Cronin[2], Lisa C. McNeill[3], Donna J. Shillington[4], Robert L. Gawthorpe[5], Richard E. Ll. Collier[6], Gino de Gelder[7], Anna Rose Golub[2], Michael R. Toomey[2], Robert K. Poirier[2], Huai-Hsuan May Huang[8,9], Marcie Purkey Phillips[10]

[1] *CNR- Institute of Environmental Geology and Geoengineering, Area della Ricerca di Roma 1, Via Salaria km 29,300, 00015 Montelibretti, RM,Italy*

[2] *Florence Bascom Geoscience Center, National Center, MS 926A, U.S. Geological Survey, 12201 Sunrise Valley Drive, Reston, VA 20192, USA*

[3] *National Oceanography Centre, Southampton, University of Southampton, Southampton SO14 3ZH, UK*

[4] *Northern Arizona University, School of Earth and Sustainability, Flagstaff, AZ, 86011*

[5] *Department of Earth Science, University of Bergen, P.O. Box 7803, N-5020 Bergen, Norway*

[6] *School of Earth and Environment, The University of Leeds, Leeds, United Kingdom*

[7] *Institut de Physique du Globe de Paris, Sorbonne Paris Cité, Université Paris Diderot, Paris, France*

[8] *Department of Paleobiology, National Museum of Natural History, Smithsonian Institution, Washington DC 20013-7012, USA*

[9] *Department of Geosciences, Princeton University, Princeton, NJ 08544, USA*

[10] *University of Texas Institute for Geophysics, Austin, TX, 78758*

ABSTRACT

Records of relative sea-level rise (RSLR) for the last deglaciation are mostly limited to coral reef records and geophysical model estimates, but observational data from regions with temperate climates is sparse. We present a new relative climatic and regional sea-level rise (RSLR) record for glacial Termination 1 (Marine Isotope Stages [MIS] 2-1) based on ostracode paleoecology from the upper 8 m of the International Ocean Discovery Program (IODP) Site M0080 collected on Expedition 381, in the Gulf of Alkyonides, eastern Corinth basin of the Mediterranean Sea. Results show a series of major faunal transitions from lacustrine (Ponto-Caspian, Lake Corinth) glacial-age assemblages to fully marine (Mediterranean) interglacial assemblages between 20

and 8 ka. During glacial and early deglacial intervals, the Gulf of Alkyonides was characterized by non-marine lacustrine conditions with episodic sediment input from coastal, saline lake environments. Relatively stable lake shoreline conditions marked by the distinctive *Tuberoloxoconcha* sp. existed from ~17.5 to 15 ka. During the peak deglacial interval, the Bølling-Allerød (B-A, ~15-13.5 ka), rapid sea-level rise is indicated by the colonization by a fully marine ostracode fauna, which persisted from 13.5 to 7.5 ka (Late Pleistocene-Early to Middle Holocene).
The transition from lacustrine to marine environments confirms that during the last glacial maximum (LGM) low sea level (-130-125 meters), the Corinth-Alkyonides depocentres were lacustrine. Marine water breached the shallow Rion and Acheloos-Cape Pappas sills, which today are currently ~50-60 m deep, separating the Mediterranean and Corinth-Alkyonides system beginning about 15 ka. Based on Alkyonides sedimentation rates, mean rates of sea-level rise during the B-A flooding of the Corinth-Alkyonides system are comparable to those obtained from coral reef SL records, at least 10-20 mm yr^{-1}. Changes in sedimentation and sill depths in this tectonically active region may have played a role in reconnection of the Mediterranean and Corinth/Alkyonides system over a prolonged period. However, the ages and scale of the faunal changes and their clear correspondence with previously published global sea-level curves and the regional sea-level curve based on deglacial land elevation changes predicted by the ICE-7G model suggests the M0080A deglacial is dominated by the glacio-eustatic sea-level rise and records details of global climate changes during Termination 1.

INTRODUCTION

During the late Quaternary, global sea level oscillated by up to ~125-130 m between glacial low stands and interglacial high stands caused by large ice sheet growth and decay. These ice volume changes are linked to orbital-scale paleoclimate variations known from benthic foraminifera oxygen isotope records (e.g., Lisiecki and Raymo 2005), when correcting for deep-sea bottom temperature changes (e.g., Lea et al., 2002; Waelbroeck et al., 2002; Elderfield et al. 2012), and can be tied to uranium-series dated coral reef terraces (Past Interglacials Working Group of PAGES, 2016). Sea-level rise during the last deglaciation, Termination I (~19-7 ka), has been documented mainly from coral reef and continental margin records summarized in Supplement Table 1 of Lambeck et al. (2014) and geophysical modeling of glacio-isostatic adjustment (GIA) (Lambeck et al. 2014, Peltier et al. 2015, 2021, Roy and Peltier 2018).

However, additional regional sea-level records are required to test these global sea-level records and glacio-isostatically corrected regional sea-level models (e.g., Roy and Peltier 2018). In 2017, IODP Expedition 381 recovered sediment core from Site M0080 (Latitude*:* 38.12000°N, Longitude*:* 23.08630°E, 348.8 m water depth) down to 534.1 mbsf from the Gulf of Alkyonides (McNeill et al. 2019a) (Figure 1). The main objective was to examine rift stratigraphy and tectonic history of this region located in the eastern part of the Corinth rift system (McNeill et al. 2019b). The Corinth-Alkyonides Gulf also contain excellent sea level and paleoclimate records due to the well-defined cyclic nature of sedimentation in the system (e.g., Collier et al. 2000, Leeder et al. 2002) (Figure 2), orbital-scale onshore and offshore sea-level records (e.g., de Gelder et al. 2019), and orbital records from the eastern Mediterranean (Konijnendijk et al. 2015). The Corinth-Alkyonides depocentres are partially closed in the west, across the Straits of Rion, by a sill which is currently 50-60m below sea level. The Corinth and Alkyonides depocentres are themselves separated by a sill 320m below sea level, in the hanging wall to the West Alkyonides Fault (Leeder et al. 2002). During glacio-eustatic lowstands, when the rift was occupied by a lake maintained at the level of the western sill, the Alkyonides depocentre remained a deep-water lake (Collier et al. 2000, Leeder et al, 2002, Leeder et al. 2005, McNeill et al. 2019b). In such complex palaeoenvironmental settings, ostracods can be particularly useful proxies, because, unlike other commonly used micropaleontological proxies such as foraminifera and nannoplankton, ostracods occur in almost all aquatic environments, from deep marine to temporary freshwater. Consequently, core M0080 offers an opportunity to examine Quaternary glacial-interglacial sea-level oscillations in detail, specifically providing insights into the pattern of sea-level rise above the level of the Rion sill during Termination I, and to test our findings against other climatic records.

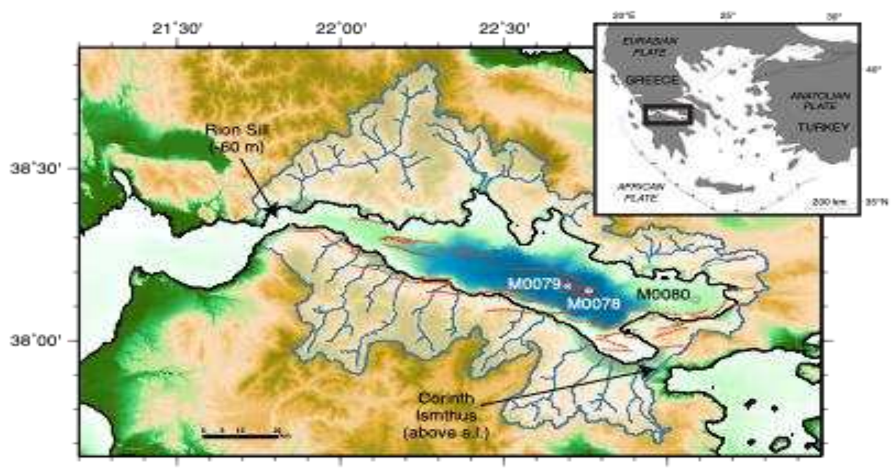

Figure 1. Map showing Gulf of Corinth/Alkyonides bathymetry, and fault distribution and location of IODP Leg 381 sites (Nixon et al., 2016 and McNeill et al., 2019a). The current study focused on core M0080A in the Gulf of Alkyonides.

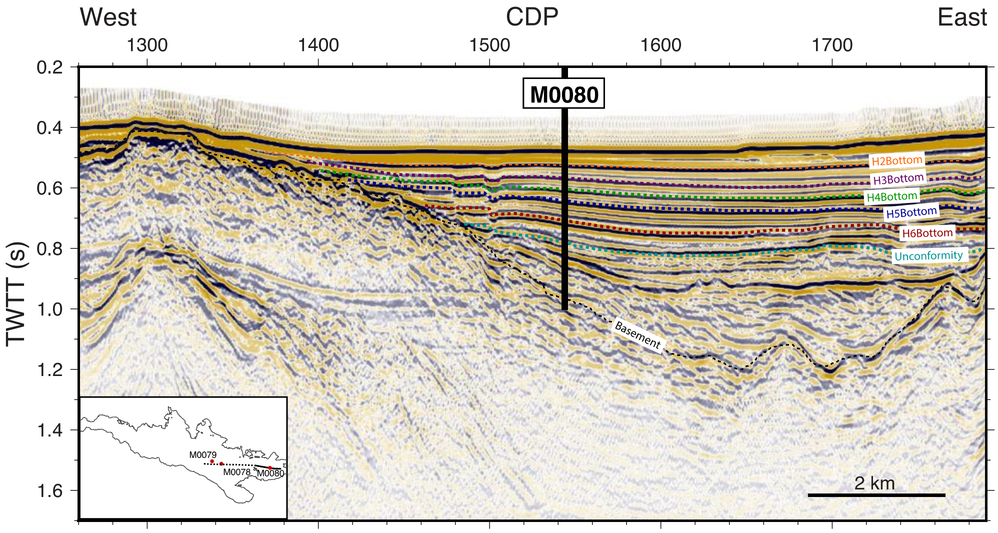

Figure 2. Seismic stratigraphy for the Gulf of Alkyonides showing location of Site M0080. The seismic line is *Maurice Ewing* Line 22 (Taylor et al., 2011) and interpretations from Nixon et al. (2016) (colored dotted lines and text). CDP = common depth point, TWT = two-way traveltime. Inset: seismic line and drill site locations.

MATERIALS & METHODS

Initially, samples from the upper 178 m of core were used for micropaleontological analyses of marine and non-marine ostracodes. Sample spacing of 0.5 to 3 m was guided by lithostratigraphy, depth to seismic reflectors H1 through H6 shown in Figure 2 (Nixon et al. 2016) and shipboard analyses of marine intervals based on foraminifera and other microfaunal groups (McNeill et al. 2019b). This information guided higher frequency sampling every 10 cm or less from the interval 8 to 3 mbsf core depth, representing Termination 1, for radiocarbon dating and focused study of the marine transgression during the last deglaciation. Sediment was processed by first washing through a 63-micron sieve and drying in an oven. Ostracodes from the > 125-micron size fraction were picked under a stereomicroscope. Ostracodes were abundant and well preserved in almost all samples. A total of 49 taxa were identified at the Consiglio Nazionale delle Ricerche, IGAG, Rome and the U. S. Geological Survey, Reston, Virginia using taxonomy and ecology from a large Mediterranean and Ponto-Caspian literature (given in Supplementary Appendix).

RESULTS

Chronostratigraphy

Preliminary shipboard calcareous nannofossil data indicate that the interval from 0 to 6.24 mbsf represents the Holocene interglacial (MIS 1), the 8.87-21.15 mbsf section is roughly 70 ka, and 35.4 mbsf is dated as MIS 7 or younger (Purkey Phillips in McNeill et al., 2019b) confirming earlier studies of the Alkyonides stratigraphy (Collier et al. 2000). It should be noted that the occurrence of *Emiliani huxleyi* down to 35.45 m may not reflect its total range as its true appearance is during a glacial period when nannofossils are not preserved (in the non-marine intervals).

An age model for the deglacial interval of the Site M0080 core was developed from 6 benthic foraminifera and 4 non-marine ostracode radiocarbon dates from the National Ocean Sciences Accelerator Mass Spectrometry (NOSAMS) facility (Table 1), collected from the 7.85 to 3.70 mbsf interval. For each date 200-300 specimens were used, with a cumulative weight ranging from ~ 2 to 8.5 mg. Additionally, two dates representing the last glacial period were obtained from organic material recovered at core depots of 8.5 and 11.26 mbsf by the Poznan Radiocarbon Laboratory. Radiocarbon dates from foraminifera were calibrated using Marine

Radiocarbon dates

Receipt #	Calib	MBSF	Material	14C-age	CMBSF	Age Err	δ13C	20-CalAge	95%	
165009 *	MARINE 20	3.7	Benthic forams	7,810	370	40	-0.46	8090	7939	8255
165011 *	MARINE 20	4.05	Benthic forams	9,820	405	50	-0.42	10607	10376	10843
165013 *	MARINE 20	5.15	Benthic forams	10,800	515	55	-0.57	12042	11788	12357
166921 *	MARINE 20	5.32	Benthic forams	10,250	532	40	-0.55	11209	11060	11389
165015 *	MARINE 20	5.7	Benthic forams	12,250	570	70	-0.25	13595	13371	13801
166920 *	MARINE 20	5.82	Benthic forams	13,300	582	45	0.02	15166	14941	15408
165017 *	IntCal20	6.65	Non-marine Ostracodes	13,800	665	95	-1.69	16744	16432	17026
166922 *	IntCal20	6.82	Non-marine Ostracodes	15,950	682	80	-0.73	19260	19042	19482
165018 *	IntCal20	7.15	Non-marine Ostracodes	14,450	715	85	0.72	17626	17362	17904
165019 *	IntCal20	7.85	Non-marine Ostracodes	16,400	785	110	0.15	19780	19530	20096
Organic material (de Gelder) radiocarbon dates										
10780		8.5	organic matter	18 010	850	100				
10803		11.26	organic matter	24 490	1126	170				

Delta R for MARINE 20 dates = 92+/-55 years

*Ten dates used in linear and Bacon age models

Mollusc dates not used in age model										
Receipt #	**Calib**	**MBSF**	**Material**	**14C-age**	**CMBSF**	**Age Err**	**δ13C**	**20-CalAge**	**95%**	
165010	MARINE 20	4	Mixed, molluc fragments	11,200	400	65	-0.65	12569	12382	12729
165012	MARINE 20	4.65	Benthics & mollusc fragments	7,100	465	35	-0.32	7404	7267	7545
165014	MARINE 20	5.6	Mollusc fragments & benthics	9,510	560	45	-1.1	10200	10007	10401
165016	MARINE 20	6.15	Mollusc fragments & benthics	11,300	615	60	-0.7	12654	12479	12798

Table 1. Summary of all the radiocarbon dates performed on different materials from core M0080.

2020 (Reimer et al. 2020), with those from ostracodes (non-marine) being calibrated via CALIB 2020 (Stuiver et al. 2021). Using these ten radiocarbon dates, we computed a linear age-depth model yielding an inferred mean sedimentation rate of 27.1 cm/kyr (S-fig. 1). A second age model incorporating four additional radiocarbon dates from mollusk fragments yielded a similar sedimentation rate (28.9 cm/kyr) but produced a lower r^2 value compared to the original age model (0.744 vs 0.927, respectively). These are most likely hemipelagic background rates for the marine interval but may represent sediment accumulation rates that include undifferentiated turbidite intervals. We chose to use the model using foraminifers and ostracodes only due to potential transport, reworking or vital effects on mollusk shells. We also computed an age model using the 10 dates using the Bacon age model (Blaauw and Christian 2011, https://chrono.qub.ac.uk/blaauw/manualBacon_2.3.pdf), which generally produced very similar ages to the foram-ostracode model (Supplement Fig S1). Although sedimentation rates in the Gulf of Alkyonides vary during glacial and interglacial periods due to tectonic and paleoclimate influences on sediment flux, our record suggests a mean sedimentation rate of about 35-37 cm kyr^{-1} for the last deglaciation and a sampling resolution of ~125 yr for the period of most rapid SLR, corresponding with the Bølling-Allerød warming event. These high sedimentation rates and high sampling resolution allow us to capture the timing of important centennial to millennial changes in deglacial inundation rates.

Faunal assemblages and taphonomy

The sedimentation in the Corinth-Alkyonides system is complex, highly variable both spatially and temporally, and subject to mixing due to downslope transport, potentially introducing artifacts within micropaleontological faunas. Three distinctive ostracod assemblages are defined, corresponding to three main different palaeoenvironments: marine, Ponto-Caspian and *Tuberoloxoconcha* assemblages (Table 2). Figure 3 shows the ostracode assemblages from Site M0080 used to infer environmental changes during the last deglacial sea-level rise in the Gulf of Alkyonides (Table 1). The shell preservation of the marine and the *Tuberoloxoconcha* group is excellent with minimal signs of physical or chemical [dissolution] alteration. For example, fine spines on the surface of *Henryhowella* are extremely well-preserved. Juvenile and adult valves and occasional articulated carapaces are present in most samples, most notably *Tuberoloxoconcha*. The Ponto-Caspian glacial lake assemblages also contain adult and juvenile valves of most species, although those of the common genus *Candona* are often broken which is expected due to its thin, relatively fragile and large size of the shells.

M80 Zones	Climate Interval**	M80 Core depth (c	Linear Age Model	Bacon Age Model	Alkyonides Gulf Environment	Faunal features	Global Sea Level *	
Marine A	Younger Dryas-E. Holocene	360-550	7929-13146	8257-12964	Fully Mediterranean Marine	Diverse Mediterranean fauna	14-12.5 ka - 20 m SLR in 1500 years	
Marine B	Late Bolling-Allerod	550-602	13146-14917	12964-14946	Initial Intermittant marine	Alternating Mediterranean/ *Tuberoloxoco*	Rapid SLR 13-15 ka, 40 mm/yr	
Tuberoloxoconcha A	Bolling-Allerod	552-600	13474-14860	13032-14890	Initial Intermittant marine	Alternating Mediterranean / *Tuberoloxoc*	Rapid SLR 14.5-14 ka, MWP-1A	
Tuberoloxoconcha B	Late Heinrich Event 1	600-672	14860-16881	14890-16847	Stable brackish	Dominant Stable *Tuberoloxoconcha*	18-16.5 ka: near stable SL, short Late H-1 SLR	
Tuberoloxoconcha C	Early Deglacial; Heinrich 1	680-790	17170-20343	17318-19748	Intermittant brackish/lacustri	*Tuberoloxoconcha* alt with Pont-Caspian	19 kyr MWP**	
Ponto-Caspian	Last Glacial Maximum	682-790	17227-20346	17151-19748	Ponto-Caspian Lake, Intermitt	Mainly Ponto-Caspian Lake, *Candona*	LGM global SL ~ -125 m	
Overlapping zones								
*See Clark et al. 2009, Lambeck et al. 2014, Peltier et al. 2015								
** See Clark et al 2012								

Table 2. Faunal zones based upon ostracod assemblages.

Figure 3 shows the ostracode assemblages from site M0080 used to infer environmental changes during the last deglacial sea level rise in the Gulf of Alyonides (Supplementary Table 1).

Given the relative base level history of the Corinth-Alkyondies depocentres (Collier et al. 2000, Leeder et al. 2005) and the present water depth at site M0080A, deposition at this site during the last deglaciation would have been at about 300-310m water depth under lacustrine conditions and up to 350m below sea level under marine conditions. The extraordinary preservation of

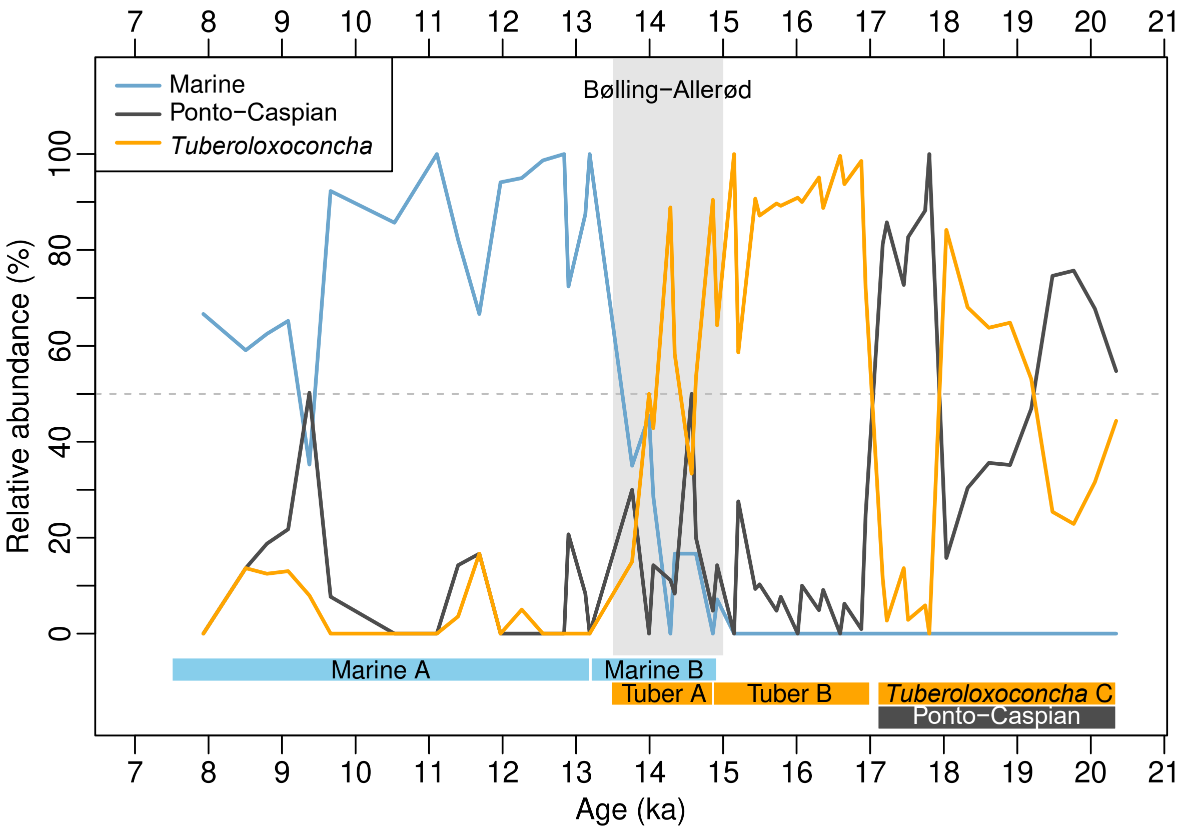

Figure 3. Major ostracode faunal zones from the 8 to 3 mbsf core depth from core M0080A. Marine (blue), Ponto-Caspian (black), and *Tuberoloxoconcha* spp. (orange) subzones are indicators of marine, lacustrine, and brackish, saline lake environments. Six faunal zones and subzones represent a progressive transition from lacustrine to fully marine environments. *Tuberoloxoconcha* spp. subzone C and Ponto-Caspian zones alternate with each other during ~20–17 ka and represent intermittent brackish and lacustrine environments, respectively. *Tuberoloxoconcha* spp. subzone B is characterized by the dominance of *Tuberoloxoconcha* (80–100%) and represents a stable coastal environment ~ 17–15 ka. *Tuberoloxoconcha* spp. subzone A and Marine subzone B partially overlap with the Bølling−Allerød warming event (14.6–12.89 ka; gray shading) and are characterized by alternating Mediterranean marine fauna and littoral brackish *Tuberoloxoconcha* species. Marine A is characterized by diverse Mediterranean marine fauna and represents a generally stable marine environment. Age model uses calibrated radiocarbon dates in Table 1 and plotted in Supplementary Figure 1. The Bølling/Allerød interstadial interval is noted.

ostracodes implies that many of these particles may have been transported out into the basin by low concentration (hypopycnal) plumes. Paralic ostracodes may have been reworked by rivers migrating or avulsing across the lagoonal and coastal environments where they were endemic, or in low-concentration plumes generated by coastal wave action. Sediment grains and ostracods would have then settled as hemipelagic particles with few grain-to grain-abrasive interactions (as opposed to being reworked by much more abrasive turbulent underflows). The active tectonic uplift of the southern coastline of the Alkyonides Gulf, at a rate of ~0.3m/kyr (Leeder et al. 2005), may have promoted rapid erosion of coastal sediments. Bathyal species may on the other hand be preserved in situ.

MIS 2-1 Transition during Termination I

Interval from 20.5 ka to 17 ka

The term Ponto-Caspian (Ponto-Caspian Zone, Figure 3) has been applied to saline lake environments of the region and distinct saline-lake faunas formed in Paratethyan basins over the last 15 million years in the eastern Mediterranean. Ponto-Caspian lakes, like the modern Caspian Sea and the Black Sea prior to Holocene marine flooding, were isolated from marine influence. These types of lakes, not in connection with sea water and characterized by inhomogeneity in ionic proportions, are called athalassic (Bayly 1969). Their ostracode fauna is highly different from that recovered in and around coastal brackish environments with marine influence (De Deckker 1981). Ponto-Caspian lakes hosted diverse ostracode faunas, often with endemic species. Those Ponto-Caspian faunas in the Corinth-Alkyonides Gulf M0080 include taxa such as *Candona*, *Amnicythere*, and certain species of *Leptocythere,* which dominated the non-marine lake phases during glacial periods.

In the Gulf of Alkyonides, dominant lacustrine and coastal assemblages characterize the glacial lake phase ~ 20-18.5 ka. These include lacustrine Ponto-Caspian assemblages and a distinct, coastal group, *Tuberoloxoncha* spp. The *Tuberoloxoconcha* genus includes interstitial, burrowing species, phytophiles or epipsammitic (living inside the surficial sandy layers) that can live in a wide range of salinities (5-34‰) in the Atlantic Ocean, as well as the Mediterranean and the Black seas (Danielopol & Bonaduce 1990, Horne, 1989, Zenina et al. 2022). They are documented in marsh environments connected to estuaries, lagoons, fine sand intertidal areas with algae, and sandy beaches, at a maximum depth of 40 m below sea level (Cabral and Loureiro, 2013; Horne et al. 2022). *Tuberoloxoconcha* spp. is very habitat-specific, living in athalassic and brackish coastal zones and thus is an excellent shoreline marker. The brief dominance of Ponto-Caspian assemblages at ~18–17 ka in the Alkyonides cores coincides with the well-known climate event known as Heinrich Event 1, although the climatic and environmental significance of Heinrich Event 1 in the Gulf of Alkyonides requires further study.

Interval from 17 ka to 15 ka

In the *Tuberoloxoconcha* spp. subzone B, this group dominates (74-99 %) the Alkyonides fauna between 670 and 600 cm core depth signifying a stable coastal environment in a glacial lake between ~ 17 and 15 ka. We interpret this as a period of nearly stable hydroclimate with minimal variability in athalassic faunas. Our radiocarbon dating supports this period being slightly younger than the period of relatively stable sea level and northern hemisphere climate from approximately 18 ka to 16.5 ka. Importantly, near-constant paleoclimate conditions imply a slowdown of deglaciation and coincides with plateaus in the Antarctic ice core deuterium (Jouzel et al., 2007) and NGRIP Greenland ice core oxygen isotope (Obrochta et al., 2014).

Interval from 15 ka to 13.2 ka

Tuberoloxoconcha spp. subzone A is characterized by rapidly decreasing percentages of this species and coincident increases of marine species from 0 % to 100 % of the assemblages

(Marine subzone B). This critical period corresponds with the period of rapid hemispheric warming and global sea level rise during the Bølling-Allerød interstadial period (B-A) ~ 15-13.5 ka discussed below.

Interval from 13.2 ka to 8 ka

Finally, the marine assemblage (Marine subzone A, Figure 3, ~ 13.2 to 8 ka) includes at least 27 species dominated by the genera *Henryhowella*, *Cytheropteron*, *Loxoconcha* and others typical of modern eastern Mediterranean faunas. There is variability in the most dominant marine species during the late deglacial and Holocene interglacial probably reflecting differences in water depth, bottom environments, and perhaps source Mediterranean faunas. However, we note that *Henryhowella sarsi* (Muller) is typically a bathyal species in the Mediterranean (Bonaduce et al. 1999), which suggests a paleodepth ~ 100-400 m, roughly similar to the modern depth of 348 m at the core site. There is a brief increase in Ponto-Caspian species at ~10-9ka which is attributed to likely reworking from older glacial sediments.

DISCUSSION

The Gulf of Alkyonides Site M 0080 allows us to examine the phases of glacial and deglacial paleoclimate and relative sea level change during Termination 1. A selection of global sea-level and paleoclimate curves during the Marine Isotope Stage (MIS) 2-1 transition are illustrated in Figure 4. In Figure 4A we show RSL estimates for the study region, which were determined by correcting the ESL record of Waelbroeck et al. (2002) for land elevation throughout Termination 1 predicted by the ICE-7G_NA (VM7) GIA model of Roy and Peltier (2018) and Peltier (2021). Figures 4B through 4F show the global sea level curves from Lambeck et al. (2014, multiple coastal sources), Waelbroeck et al. (2002, oxygen isotope ice volume corrected for bottom temperatures), and Barbados (Peltier et al. 2006, 2008), as well as the North Greenland Ice Core oxygen isotope (updated by Obrachta et al. 2014) and Antarctica deuterium (Jouzel et al. 2007) paleoclimate.

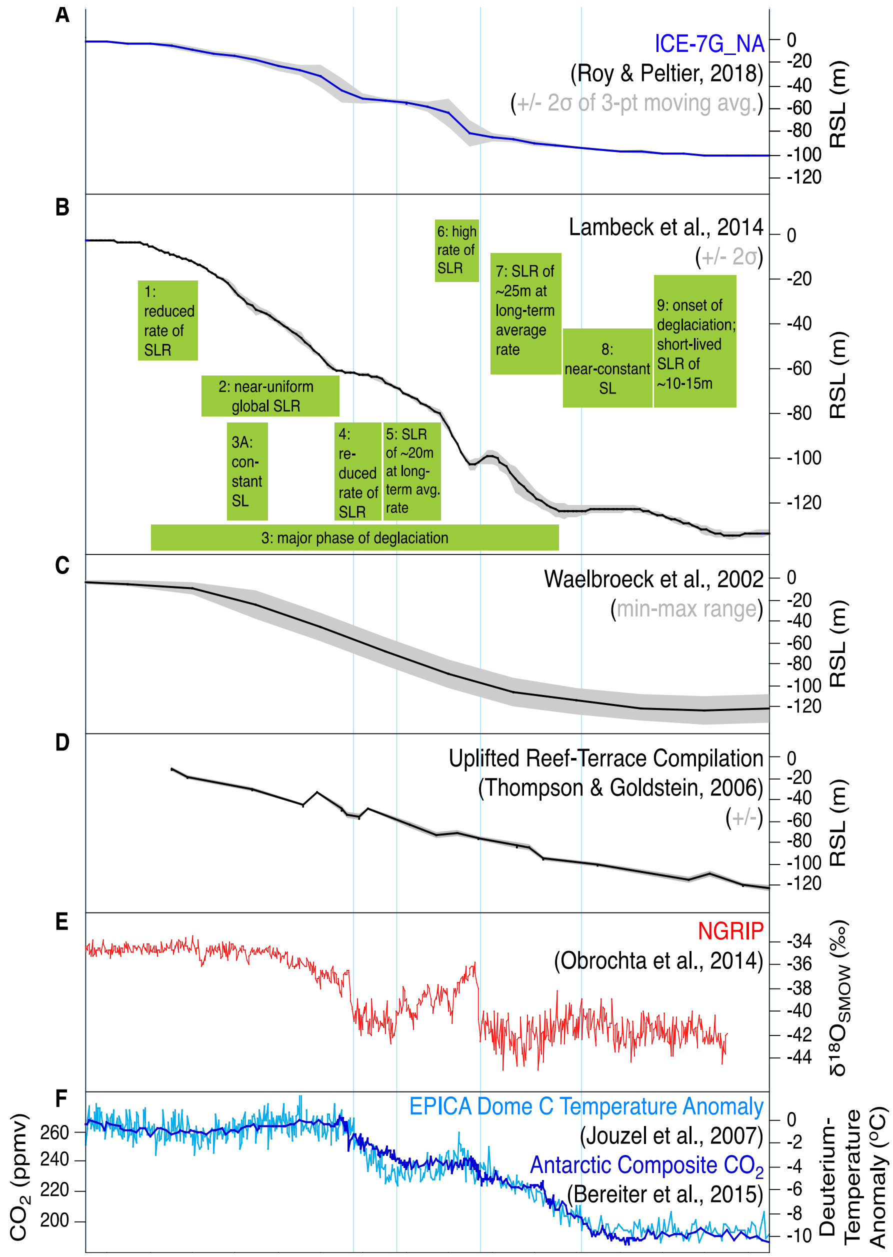

Figure 4. Global sea level and climatic events during the Marine Isotope Stage (MIS) 2-1 transition. A. ICE-7G_NA regional sea level model of Roy and Peltier (2018) for the Rion and Acheloos-Cape Pappas sill region separating the Corinth-Alkyonides system from the Mediterranean. B. Global sea-level curve from Lambeck et al. (2014). Green boxes indicate stages of RSL changes (Lambeck

et al. 2014). C. Global sea-level curve from Waelbroeck et al. (2002) based on dep-sea foraminiferal oxygen isotope records corrected for deep bottom water temperatures. D. Uplifted coral reef-terrace compilation sea-level record from Thompson & Goldstein (2006). North GRIP Greenland oxygen isotope record showing major northern hemisphere deglacial events (Andersen et al., 2004, Rasmussen et al., 2006, Obrochta et al., 2014). F. Deuterium-derived temperature anomaly record from EPICA Dome C ice core (light blue), Antarctica (Jouzel et al., 2004, 2007), and the Antarctic composite CO_2 record of Bereiter et al. (2015). Abbreviations: YD=Younger Dryas, ACR=Antarctic Cold Reversal, B-A= Bølling-Allerød, H1= Heinrich Event 1.

The relationships between the ostracode faunal patterns and the periods of global sea level change are illustrated in Figure 5. At the onset of deglaciation (~21-19 ka BP), there is a short-lived global sea-level rise (SLR) of ~10–15 m (Clark et al., 1996; Lambeck et al., 2014), which is not seen in the continuing lacustrine environment of the Alkyonides. Subsequently, Lambeck et al. (2014) documented a ~25-m global SLR at ~16.5–15 ka BP that was the main phase of deglaciation. The Alkyonides faunas also suggest a rapid transition from saline lake to fully marine environments beginning about 15 ka and accelerating until 13.5 ka. This sea-level rise coincides with the Bølling-Allerød interstadial period (B-A), an abrupt northern hemisphere warming event during the deglaciation, corresponding with Meltwater Pulse 1A. This faunal shift from non-marine and coastal species to near 100% marine ostracode species in the Alkyonides record (Marine-Mediterranean fauna, Figures 3, 5) thus appears to be coincident with the abrupt hemispheric-wide B-A warming identified in many paleoclimate records (Figure 4). This transition represents the most rapid global SLR rate of the last deglaciation, lasting about 500 years, and it is most likely that the B-A sea-level rise event in the Gulf of Alkyonides resulted in the full breaching of the Rion and Acheloos-Cape Pappas sills at the western entrance to the Gulf of Corinth and hence the Gulf of Alkyonides (Figure 5).

Lambeck et al (2014) estimated a total SLR of ~20 m from ~14 to ~12.5 ka BP, a ~1,500-year period when marine species dominate the Site M0080 record. A reduced rate of SLR

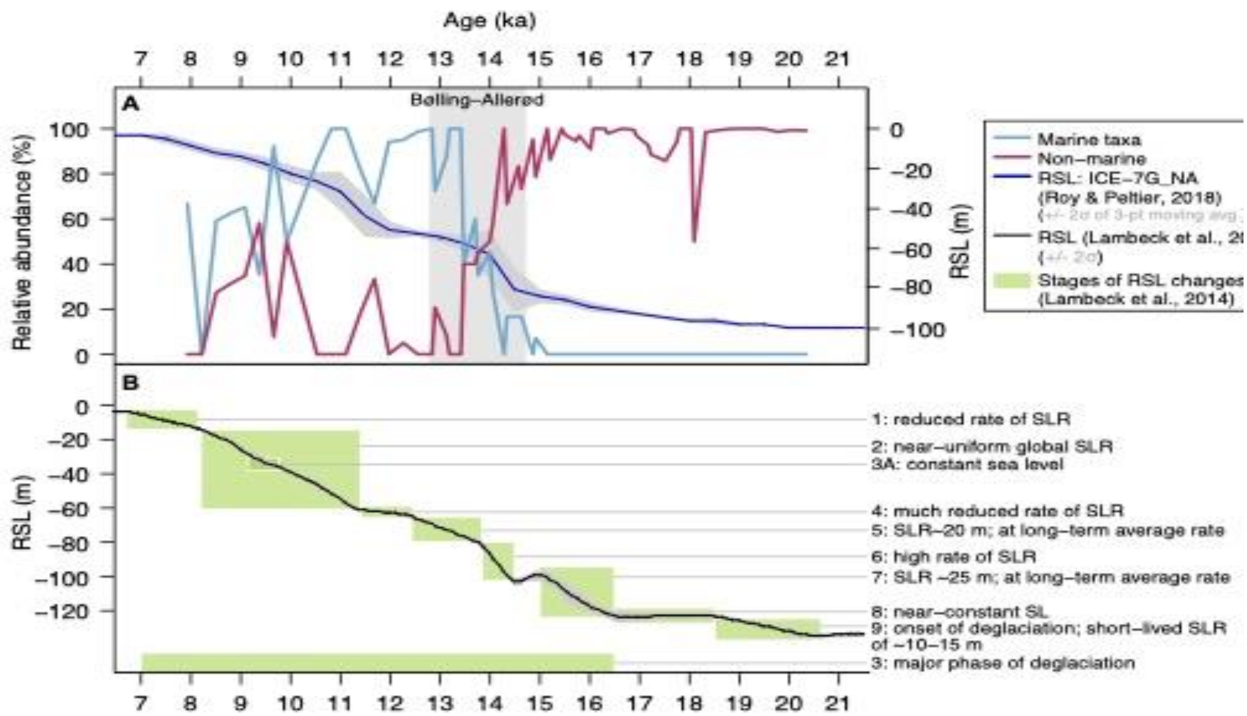

Figure 5. A. M0080 faunal zones with characteristic Alkyonides Gulf paleoenvironments (Table 2) plotted against ICE-7G_NA regional sea level curve. B. Global sea-level curve from Lambeck et al. (2014) with global sea-level trends identified throughout the deglacial interval.

from ~12.5–11.5 ka BP, near-uniform global SLR from ~11.4 to 8.2 ka BP, and reduced SLR rate from 8.2 to 6.7 ka BP do not appear to be reflected in the ostracode faunas as the Corinth-Alkyonides Gulf system had become fully marine.

CONCLUSIONS

The non-marine to marine transition in Alkyonides ostracode assemblages centered on 15-13.5 ka demonstrate that, despite the active tectonic setting, the primary forcing of sedimentation and paleoenvironments in the Gulf of Alkyonides are global glacio-eustatic sea level cycles driven by global ice volume. As with deep-sea isotope records of glacial terminations, intervals of deglaciation were extremely abrupt, occurring over 1-3 meters of section. These results confirm interpretations of multiple previous studies (e.g., Nixon et al., 2016, references therein) that Alkyonides seismic stratigraphy reflects mid to late Quaternary sea-level oscillations.

Due to the high sedimentation rate, the Alkyonides paleo-sea level record provides a unique test of global sea-level records from geophysical models and reveals new details about the last deglaciation. These include:

1. Fluctuating non-marine, saline lake environments from ~20 ka to 15 ka, with a possible signal for Heinrich Event 1 near ~18-17 ka;
2. A ~500-1000 period of stable lacustrine environments ~16.5 to 15.5 ka, slightly younger than the stable climate shown in the sea level record of Lambeck et al. (2014) and coincident with plateaus in Antarctic and Greenland paleoclimate curves;
3. The well-known large (~20 m), rapid (< 500 years), SLR during the Bølling−Allerød interstadial centered on ~14.5 ka corresponding with Meltwater Pulse (MWP) 1A;

4. Complete flooding of the Alkyonides Gulf by the Younger Dryas and early Holocene including the post-YD MWP 1B (13.3-10 ka).

ACKNOWLEDGMENTS

We are grateful to the shipboard scientific staff and crew of the *Fugro Synergy*, mission-specific platform, for the initial work on IODP 381 Site M0080 and Holger Kuhlmann and the Bremen, Germany IODP repository for assistance in sampling the core. IM was funded by the CNR-Short Term Mobility Program 2018 and TMC, ARG, RP, and MRT by the USGS Climate Research & Development Program. Any use of trade, firm, or product names is for descriptive purposes only and does not imply endorsement by the U.S. Government.

REFERENCES

Andersen, K., Azuma, N., Barnola, J.M., Bigler, M., Biscaye, P., Caillon, N., Chappellaz, J., Clausen, H., Dahl-Jensen, D., Fischer, H., Flückiger, J., & Fritzsche, D., Fujii, Y., Goto-Azuma, K., Grønvold, K., Gundestrup, N., Hansson, M., Huber, C., Hvidberg, C., and White, J., 2004, High-resolution record of Northern Hemisphere climate extending into the last interglacial period. *Nature*, v. 431, p. 147-51, doi: 10.1038/nature02805.

Bayly, I. A. E., 1969. Symposium on 'Salt and Brackish Inland Waters'. Introductory Comments. Verh. Int. Ver. Limnol. 17: 419–420.

Bereiter, B., Sarah Eggleston, Jochen Schmitt, Christoph Nehrbass-Ahles, Thomas F. Stocker, Hubertus Fischer, Sepp Kipfstuhl, Jerome Chappellaz, 2015. Revision of the EPICA Dome C CO_2 record from 800 to 600 kyr before present. *Geophysical Research*

Letters 42 (2). doi: 10.1002/2014GL061957.

Blaauw, M. and Christen, J.A., 2011. Flexible paleoclimate age-depth models using an autoregressive gamma process. *Bayesian Analysis,* 6, 457-474.

Blunier, T., and Brook, E.J., 2001, Timing of millennial-scale climate change in Antarctica and Greenland during the last glacial period. *Science*, 291, p. 109-112. doi: 10.1126/science.291.5501.109

Blunier, T., and Brook, E.J., 2001, Synchronization of the Byrd and Greenland (GISP2/GRIP) Records, IGBP PAGES/World Data Center-A for Paleoclimatology, Data Contribution Series #2001-003, NOAA/NGDC Paleoclimatology Program, Boulder, CO, USA.

Cabral M.C. and Loureiro I.M. 2013. Overview of Recent and Holocene ostracods (Crustacea) from brackish and marine environments of Portugal. *Journal of Micropalaeontology*, 32: 135–159. doi: 10.1144/jmpaleo2012-019

Clark, P.U., and Huybers, P., 2009, Interglacial and future sea level. *Nature*, 462, no. 7275, p. 856-857, doi:10.1038/462856a.

Collier, R.E., Leeder, M.R., Trout, M., Ferentinos, G., Lyberis, E. and Papatheodorou, G., 2000. High sediment yields and cool, wet winters: Test of last glacial paleoclimates in the northern Mediterranean. *Geology*, *28*(11), pp.999-1002. doi: 10.1130/0091-7613(2000)28<999:HSYACW>2.0.CO;2

Danielopol, D.L., and Bonaduce, G., 1990, The colonization of subsurface habitats by the Loxoconchidae Sars and Psammocytheridae Klie, *in* Whatley, R., and Maybury, C., eds., Ostracoda and Global Events: Chapman and Hall, London, p. 437-458.

De Deckker, P., 1981. Ostracods of athalassic saline lakes. A review. *Hydrobiologia* 81: 131–144.

Elderfield, H., Ferretti, P., Greaves, M., Crowhurst, S., McCave, I.N., Hodell, D., and Piotrowski, A.M., 2012, Evolution of Ocean Temperature and Ice Volume Through the Mid-Pleistocene Climate Transition. *Science*, v. 337, no. 6095, p. 704–709, doi: 10.1126/science.1221294

Hodell, D.A., et al., 2010, North Atlantic IODP U1308 Middle Pleistocene Heinrich Events Data, IGBP PAGES/World Data Center for Paleoclimatology, Data Contribution Series # 2010-067, NOAA/NCDC Paleoclimatology Program, Boulder CO, USA.

Hodell, D.A., Channell, J.E.T., Curtis, J.H., Romero, O.E., and Röhl, U., 2008, Onset of "Hudson Strait" Heinrich events in the eastern North Atlantic at the end of the middle Pleistocene transition (~640 ka)?. *Paleoceanography*, v. 23, PA4218, doi:10.1029/2008PA001591.

Horne, D.J. 1989. On *Tuberoloxoconcha atlantica* Horne sp. nov. Stereo-Atlas of Ostracod Shells 16 (17), 73–76.

Horne, D.J., Cabral, M.C., Fatela, F. and Radl, M., 2022. Salt marsh ostracods on European Atlantic and North Sea coasts: Aspects of macroecology, palaeoecology, biogeography, macroevolution and conservation. *Marine Micropaleontology*, 174, p.101975. doi: 10.1016/j.marmicro.2021.101975

Jouzel, J., Masson-Delmotte, V., Cattani, O., Dreyfus, G., Falourd, S., Hoffmann, G., Minster, B., Nouet, J., Barnola, J. M., Chappellaz, J., Fischer, H., Gallet, J.C., Johnsen, S., Leuenberger, M., Loulergue, L., Luethi, D., Oerter, H., Parrenin, F., Raisbeck, G., Raynaud, D., Schilt, A., Schwander, J., Selmo, E., Souchez, R., Spahni, R., Stauffer, B., Steffensen, J.P., Stenni, B., Stocker, T.F., Tison, J.L., Werner, M., and Wolff, E.W., 2007, Orbital and Millennial Antarctic Climate Variability over the Past 800,000 Years.

Science, 317, no. 5839, p.793-797. doi: 10.1126/science.1141038

Kindler, P., Guillevic, M., Baumgartner, M., Schwander, J., Landais, A., and Leuenberger, M., 2014, Temperature reconstruction from 10 to 120 kyr b2k from the NGRIP ice core. *Climate of the Past*, 10, p. 887-902, doi:10.5194/cp-10-887-2014.

Konijnendijk, T. Y. M., M. Ziegler, L. J. Lourens. 2015. On the timing and forcing mechanisms of late Pleistocene glacial terminations: Insights from a new high-resolution benthic stable oxygen isotope record of the eastern Mediterranean. *Quaternary Science Reviews,* 129:308-320. doi: 10.1016/j.quascirev.2015.10.005

Lambeck, K., Rouby, H., Purcell, A., Sun, Y., and Sambridge, M., 2014, Sea level and global ice volumes from the Last Glacial Maximum to the Holocene. *Proceedings of the National Academy of Sciences*, v. 111, no. 43, p. 15296–15303. doi: 10.1073/pnas.1411762111

Leeder, M.R., Collier, R.L., Aziz, L.A., Trout, M., Ferentinos, G., Papatheodorou, G. and Lyberis, E., 2002. Tectono-sedimentary processes along an active marine/lacustrine half-graben margin: Alkyonides Gulf, E. Gulf of Corinth, Greece. *Basin Research*, *14*(1), pp.25-41. doi: 10.1046/j.1365-2117.2002.00164.x

Leeder, M.R., Portman, C., Andrews, J.E., Collier, R.E.Ll., Finch, E., Gawthorpe, R.L., McNeill, L.C., Perez-Arlucea, M. & Rowe, P., 2005. Normal faulting and crustal deformation, Alkyonides Gulf and Perachora peninsula, eastern Gulf of Corinth rift basin, Greece. *Journal of the Geological Society, London*, 162, 549-561. doi:10.1144/0016-764904-075.

Lisiecki, L.E., and Raymo, M.E., 2012, Atlantic and Pacific 800 KYr Benthic d18O Stacks: IGBP PAGES/World Data Center for Paleoclimatology, Data Contribution Series # 2012-115, NOAA/NCDC Paleoclimatology Program, Boulder, CO, USA.

Lisiecki, L.E., and Raymo, M.E., 2009, Diachronous benthic d18O responses during late

Pleistocene terminations. *Paleoceanography*, 24, PA3210, doi:10.1029/2009PA001732.

McNeill, L.C., Shillington, D.J., Carter, G.D.O., and the Expedition 381 Participants, 2019a. *Corinth Active Rift Development*. Proceedings of the Inter- national Ocean Discovery Program, 381: College Station, TX (International Ocean Discovery Program). doi: 10.14379/iodp.proc.381.2019

McNeill, L.C., Shillington, D.J., Carter, G.D.O., Everest, J.D., Gawthorpe, R.L., Miller, C., Phillips, M.P., et al., 2019b. High-resolution record reveals climate-driven environmental and sedimentary changes in an active rift. *Scientific Reports*, 9:3116. doi: 10.1038/s41598-019-40022-w

Obrochta, S.P., Yokoyama, Y., Moren, J., and Crowley, T.J., 2014, Conversion of GISP2-based sediment core age models to the GICC05 extended chronology. *Quaternary Geochronology*, v. 20, p. 1-7, doi: 10.1016/j.quageo.2013.09.001.

Past Interglacials Working Group of PAGES. 2016. Interglacials of the last 800,000 years. Reviews of Geophysics 54, 162-219, doi:10.1002/2015RG000482.

Peltier, W. R., Argus, D. F., and Drummond, R., 2015, Space geodesy constrains ice age terminal deglaciation: The global ICE-6G_C (VM5a) model: *J. Geophysical Research Solid Earth*, 120, p. 450–487, doi:10.1002/2014JB011176.

Peltier, W.R., and Fairbanks, R.G., 2008, Barbados coral extended Last Glacial Maximum sea level record, IGBP PAGES/World Data Center for Paleoclimatology, Data Contribution Series # 2008-101, NOAA/NCDC Paleoclimatology Program, Boulder, CO, USA.

Peltier, W.R., and Fairbanks, R.G., 2006, Global glacial ice volume and Last Glacial Maximum duration from an extended Barbados sea level record. *Quaternary Science Reviews*, 25, p. 3322-3337, doi: 10.1016/j.quascirev.2006.04.010.

Peltier, W.R., Argus, D.F. and Drummond, R. (2018) Comment on "An Assessment of the ICE-6G_C (VM5a) Glacial Isostatic Adjustment Model" by Purcell et al. *J. Geophysical Research Solid Earth*, 123, 2019-2018, doi:10.1002/2016JB013844.

Peltier, W. R. 2021. https://www.atmosp.physics.utoronto.ca/~peltier/data.php.

Rasmussen, S. O., Andersen, K. K., Svensson, Anders M; Steffensen, Jørgen Peder; Vinther, Bo Møllesøe; Clausen, Henrik Brink; Siggaard-Andersen, Marie-Louise; Johnsen, Sigfús Jóhann; Larsen, L B; Dahl-Jensen, Dorthe; Bigler, Matthias; Röthlisberger, Regine; Fischer, Hubertus; Goto-Azuma, Kumiko; Hansson, Margareta E; Ruth, Urs (2006): A new Greenland ice core chronology for the last glacial termination. *Journal of Geophysical Research Atmospheres*, 111, D06102. doi: 10.1594/PANGAEA.586838

Reimer, P. et al. 2020. The IntCal20 Northern Hemisphere Radiocarbon Age Calibration Curve (0–55 cal kBP). *Radiocarbon*, 62, 4. 725 – 757. doi: 10.1017/RDC.2020.41

Roy, K., & Peltier, W. R., 2018. Relative sea level in the Western Mediterranean basin: A regional test of the ICE-7G_NA (VM7) model and a constraint on Late Holocene Antarctic deglaciation. *Quaternary Science Reviews*, 183, 76-87, doi:10.1016/j.quascirev.2017.12.021.

Stuiver, M., Reimer, P.J., and Reimer, R.W., 2021, CALIB 8.2 [WWW program] at http://calib.org.

Thompson, W.G., and Goldstein, S.L., 2006, A radiometric calibration of the SPECMAP timescale. *Quaternary Science Reviews*, 25, 3207-3215. doi: 10.1016/j.quascirev.2006.02.007

Thornalley, D.J.R., Elderfield, H., and McCave, I.N., 2010, Intermediate and Deep Water

Paleoceanography of the Northern North Atlantic Over the Past 21,000 years. *Paleoceanography*, 25, PA1211, doi: 10.1029/2009PA001833.

Veres, D., Bazin, L., Landais, A., Toyé Mahamadou Kele, H., Lemieux-Dudon, B., Parrenin, F., Martinerie, P., Blayo, E., Blunier, Capron, E., Chappellaz, J., Rasmussen, S.O., Severi, M., Svensson, A., Vinther, B., and Wolff, E.W., 2013, The Antarctic ice core chronology (AICC2012): an optimized multi-parameter and multi-site dating approach for the last 120 thousand years. *Climate of the Past*, 9, p. 1733-1748, doi: 10.5194/cp-9-1733-2013.

Waelbroeck, C., L.Labeyrie, E. Michel, J.C. Duplessy, J.F. McManus, K. Lambeck, E. Balbon, M. Labracherie. 2002. Sea-level and deep water temperature changes derived from benthic foraminifera isotopic records. *Quaternary Science Reviews*, 21, 295–305. doi: 10.1016/S0277-3791(01)00101-9

Zenina, M.A., Kolyuchkina, G.A., Murdmaa, I.O., Aliev, R., Borisov, D.G., Dorokhova, E.V. and Zatsepin, A.G., 2022. Ostracod assemblages from the Golubaya (Rybatskaya) Bay area on the outer northeastern Black Sea shelf over the last 300 years. *Marine Micropaleontology*, 174, p.102129. doi: 10.1016/j.marmicro.2022.102129

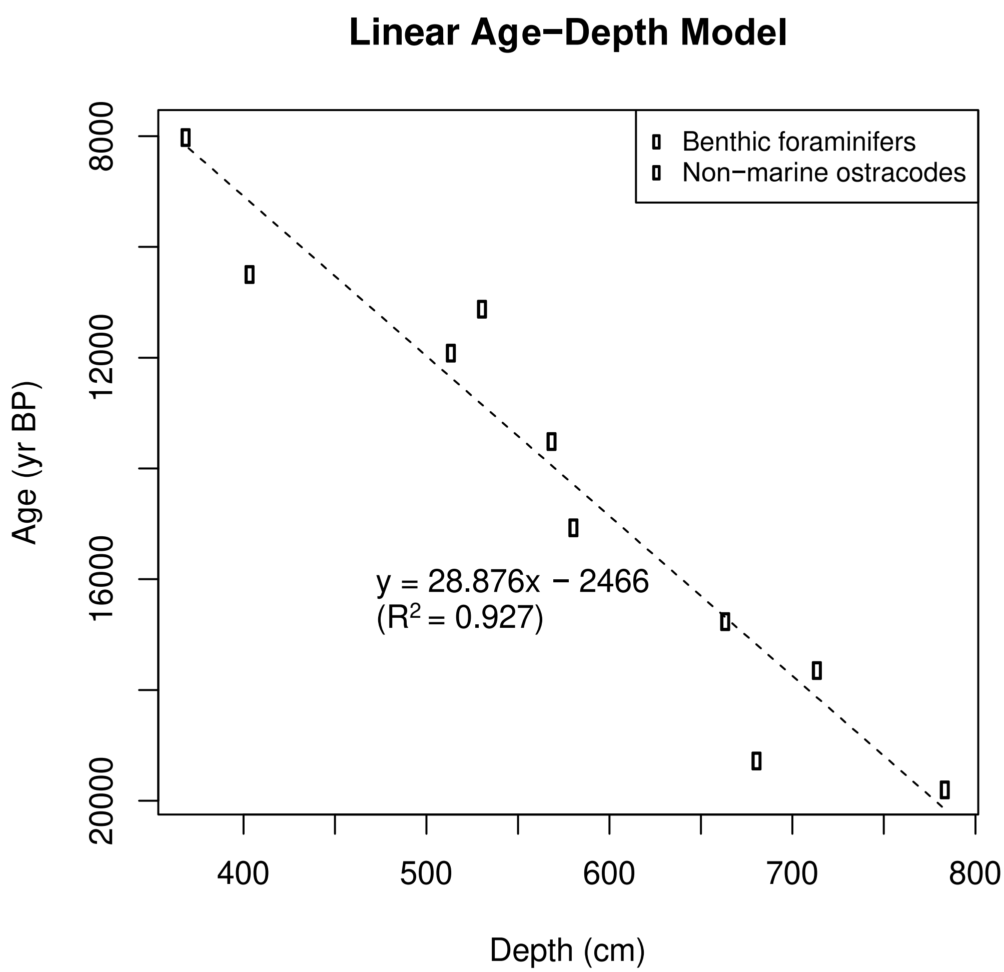

Supplementary Figure 1. Linear age depth model of M0080.